SAE TECHNICAL PAPER SERIES

2008-01-1228

Stability and Control Considerations of Vehicle-Trailer Combination

Aleksander Hac, Daniel Fulk and Hsien Chen
Delphi Corporation

Reprinted From: Brake Technology, 2008 (SP-2188)

ISBN 978-0-7680-1631-4

9 780768 016314

**2008 World Congress
Detroit, Michigan
April 14-17, 2008**

SAE International™

400 Commonwealth Drive, Warrendale, PA 15096-0001 U.S.A. Tel: (724) 776-4841 Fax: (724) 776-0790 Web: www.sae.org

All SAE papers, standards, and selected books are abstracted and indexed in the Global Mobility Database.

ISSN 0148-7191

Printed in USA

2008-01-1228

Stability and Control Considerations of Vehicle-Trailer Combination

Aleksander Hac, Daniel Fulk and Hsien Chen
Delphi Corporation

ABSTRACT

In this paper, dynamics and stability of an articulated vehicle in the yaw plane are examined through analysis, simulations, and vehicle testing. Control of a vehicle-trailer combination using active braking of the towing vehicle is discussed. A linear analytical model describing lateral and yaw motions of a vehicle-trailer combination is used to study the effects of parameter variations of the trailer on the dynamic stability of the system and limitations of different control strategies.

The results predicted by the analytical model are confirmed by testing using a vehicle with a trailer in several configurations. Design of the trailer makes it possible to vary several critical parameters of the trailer. The test data for vehicle with trailer in different configurations is used to validate the detailed non-linear simulation model of the vehicle-trailer combination. Analysis and the simulation model are used to examine the advantages and limitations of two active brake control methods: the uniform braking and the direct yaw moment (DYM) control of the towing vehicle.

INTRODUCTION

Handling behavior of articulated vehicles is more complex and less predictable than that of non-articulated vehicles. This poses challenges to non-expert drivers of light vehicles, who occasionally tow recreational trailers and may not have good understanding of dynamic complexities of a vehicle-trailer combination. The task of controlling the vehicle becomes the most difficult when the system becomes unstable. Apart from rollover, which is not discussed in this paper, the articulated vehicle may experience two types of instability in the yaw plane. The first one is a divergent instability such as jackknifing, in which the hitch angle increases without experiencing oscillations. This occurs when, at a particular operating condition, the understeer gradient of a vehicle-trailer combination becomes negative and the speed is above critical velocity. The second type is dynamic in nature and may lead to oscillatory response with increasing amplitude known as snaking or sway.

The influences of physical parameters of the vehicle and trailer on both types of instability have been investigated in detail using both validated analytical models and vehicle testing [1-6]. It has been shown [2, 5] that the divergent type of instability depends only on the parameters of the towing vehicle and on the vertical hitch load. The latter is affected by the trailer mass and the location of the trailer center of gravity in the longitudinal direction. Reducing the hitch load, or equivalently moving the trailer center of gravity rearward, improves the stability margin with respect to divergent motion. In contrast, stability with respect to the snaking motion depends on the parameters of both the towing vehicle and the trailer. More specifically, the system becomes unstable beyond a certain speed. This speed decreases, thus rendering the system less stable, as: 1) the mass of the trailer (relative to the vehicle's mass) increases, 2) the center of gravity of the trailer moves rearward, 3) the moment of inertia of the trailer increases, 4) cornering stiffness of trailer tires decreases, 5) cornering stiffness of the vehicle's rear tires decreases 6) the distance from the vehicle rear axle to the hitch point increases, 7) vehicle wheelbase decreases. Even for a specific vehicle-trailer combination, most of these parameters can be greatly altered by changing parameters that are in control of the user, such as weight distribution or tire type and tire pressure. Hence, stability of the vehicle-trailer combination cannot be guaranteed by selecting the passive design parameters, thus necessitating an active control approach.

Several active control methods have been proposed to improve handling and stability of a vehicle-trailer combination. For example, active rear steering of the towing vehicle was considered by Kageyame and Nagai [7] and active front and rear steering by Deng et al. [8]. Active control of trailer braking was investigated by Lugner et al. [9] and by Fernandez and Sharp [10], while Kimbrough et al. [11] considered active control of both vehicle and trailer braking. Aside from active vehicle brake control, these types of systems are seldom available in production vehicles or trailers. Furthermore, the proposed control strategies typically required a prior knowledge of trailer parameters and the variables describing trailer states (e.g. hitch angle, rate, trailer yaw rate or lateral acceleration of trailer center of gravity) which necessitated

additional sensors. More recently, cost effective solutions to improve stability and handling of vehicle-trailer combinations have been proposed and implemented by utilizing only brake actuators and sensors from the towing vehicle's electronic stability control (ESC) system. In essence, two control methods have been considered: one is a symmetric braking of the towing vehicle with the objective of bringing the vehicle speed below the critical speed (e.g. [12]); the second is control of the yaw moment of the towing vehicle via asymmetric braking [13]. Since no direct feed-back information about the trailer motion or even knowledge of trailer parameters is available, maintaining robustness of the control method with respect to variation in trailer parameters is one of the most important issues for systems intended for production.

In this paper, dynamics, stability, and stabilizing control of the articulated vehicle is investigated using first an analytical model and then a combination of testing and full-vehicle simulations.

ANALYTICAL MODEL OF VEHICLE-TRAILER COMBINATION

For the purpose of studying the yaw plane dynamics of the vehicle-trailer combination, a single track 4-th order model illustrated in Figure 1 is selected. It is the simplest model, which describes both types of instabilities and permits studying of the effects of system parameters and different control strategies on the dynamic behavior of the system. Nearly identical models have been considered in the past [1, 3, 5, 6] and have been shown to represent the handling dynamics very well and to achieve excellent match between the values predicted by the model and the test results.

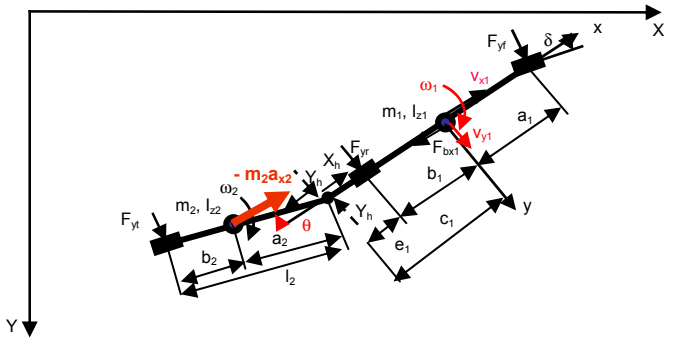

Figure 1: Simplified Model of Vehicle with Trailer in the Yaw Plane

In the model, the tires of each axle are represented as a single tire. The front wheel steering angle, δ, the hitch angle, θ, and the tire slip angles are assumed to be small. In addition, the effects of aerodynamic drag forces and deceleration on lateral dynamics are ignored. In the figure, m_1 and m_2 are the masses of the vehicle and the trailer, respectively, I_{z1} and I_{z2} are the yaw moments of inertia of the vehicle and the trailer about the respective yaw axes passing through the centers of mass. The symbols a_1 and b_1 are the distances of the vehicle front and rear axle to the center of mass, e_1 is the distance of the rear axle of the vehicle to the hitch point and $c_1 = b_1 + e_1$ is the distance of the hitch point to the vehicle center of mass. Symbols a_2 and b_2 denote the distances of the trailer center of mass to the hitch point and trailer axle, respectively, and $l_2 = a_2 + b_2$ is the distance of the trailer axle to the hitch point. The yaw rates of the vehicle and trailer are denoted by ω_1 and ω_2, respectively, and lateral velocities at their centers of mass are v_{y1} and v_{y2}, respectively. Under the small angle assumption, the longitudinal velocities of vehicle and trailer are the same $v_{x1} = v_{x2} = v_x$ and are denoted by v_x. F_{yf}, F_{yr} and F_{yt} are the lateral tire forces per axle acting at front and rear axles of the vehicle and the trailer axle, respectively. Y_h represents the hitch force in the lateral direction. Additionally, the vehicle may be subjected to the yaw moment ΔM_{z1} resulting from active asymmetric braking of the towing vehicle, which is considered the control input. Under the above conditions and assumptions, the equations of lateral and yaw motions of the vehicle and trailer are:

$$m_1 a_{y1} = F_{yf} + F_{yr} - Y_h \tag{1a}$$

$$I_{z1}\dot{\omega}_1 = F_{yf} a_1 - F_{yr} b_1 + Y_h c_1 + \Delta M_{z1} \tag{1b}$$

$$m_2 a_{y2} = Y_h + F_{yt} \tag{1c}$$

$$I_{z2}\dot{\omega}_2 = Y_h a_2 - F_{yt} b_2 \tag{1d}$$

Here, a_{y1} and a_{y2} are the lateral accelerations at the vehicle and trailer centers of mass. The following kinematic relationships hold:

$$\omega_2 = \omega_1 + \dot{\theta} \tag{2a}$$

$$a_{y1} = \dot{v}_{y1} + v_x \omega_1 \tag{2b}$$

$$a_{y2} = \dot{v}_{y1} + v_x \omega_1 - c_1 \dot{\omega}_1 - a_2 \left(\dot{\omega}_1 + \ddot{\theta}\right) \tag{2c}$$

The tire forces per axle are assumed to be proportional to the tire slip angles:

$$F_{yf} = -C_{yf}\alpha_f = -C_{yf}\left(\frac{v_{y1} + a_1\omega_1}{v_x} - \delta\right) \tag{3a}$$

$$F_{yr} = -C_{yr}\alpha_r = -C_{yr}\frac{v_{y1} - b_1\omega_1}{v_x} \tag{3b}$$

$$F_{yt} = -C_{yt}\alpha_t = -C_{yt}\left(\frac{v_{y1} - (c_1 + l_2)\omega_1 - l_2\theta}{v_x} - \theta\right) \tag{3c}$$

C_{yf}, C_{yr}, and C_{yt} denote the cornering stiffness values for the tires of the vehicle's front axle, rear axle and the trailer axle, respectively. Combining equations (1) through (3) yields a system of linear equations, which is written in a matrix form:

$$\mathbf{M}\dot{\mathbf{x}} = \mathbf{D}(v_x)\mathbf{x} + \mathbf{E}u + \mathbf{F}\delta \tag{4}$$

M, **D**, **E,** and **F** are the system matrices which are given in the Appendix. While matrices **M**, **E,** and **F** are

constant, matrix **D** is a function of vehicle speed, v_x. The state vector, **x**, and the control input, u, are given by

$$\mathbf{x} = \begin{bmatrix} v_{y1} & \omega_1 & \dot{\theta} & \theta \end{bmatrix}^T, \qquad u = \Delta M_{z1} \tag{5}$$

By pre-multiplying equation (4) on both sides by $\mathbf{M}^{-1}$, the state equation is obtained

$$\dot{\mathbf{x}} = \mathbf{A}(v_x)\mathbf{x} + \mathbf{B}u + \mathbf{G}\delta \tag{6}$$

where

$$\mathbf{A}(v_x) = \mathbf{M}^{-1}\mathbf{D}(v_x), \quad \mathbf{B} = \mathbf{M}^{-1}\mathbf{E}, \quad \mathbf{G} = \mathbf{M}^{-1}\mathbf{F} \tag{7}$$

Matrix **A** is a function of vehicle speed, v_x, while matrices **B** and **G** are constant.

It is known that the linear bicycle model of a vehicle without a trailer is described by the state equation of the same form as equation (6), specifically

$$\dot{\mathbf{x}}_\mathbf{v} = \mathbf{A}_\mathbf{v}(v_x)\mathbf{x}_\mathbf{v} + \mathbf{B}_\mathbf{v}u_v + \mathbf{G}_\mathbf{v}\delta \tag{8}$$

The matrices in equation (8) are given in the Appendix; the control input is the same as before and the state vector is

$$\mathbf{x}_\mathbf{v} = \begin{bmatrix} v_{y1} & \omega_1 \end{bmatrix}^T \tag{9}$$

The analytical model of a vehicle-trailer combination described here is used primarily to study the effect of vehicle and trailer parameters on the stability of the system at the onset of potential instability, when amplitudes of motion are small and the linear assumptions are approximately satisfied. While extensions of the model are possible by employing nonlinear tire models and avoiding the small angle assumption, in this paper a combination of vehicle testing and simulations based on a nonlinear full vehicle with trailer model are used to validate the analytical results.

STABILITY ANALYSIS

In this section, stability of the vehicle-trailer combination is investigated using the model described in the previous section. Although the concept of stability appears intuitively obvious, it is necessary to make two important points. First, any system of at least the 2nd order may experience two types of instability: a static or divergent type of instability, in which the variables describing the system increase exponentially in magnitude without oscillations and a "dynamic" instability in which the variables experience oscillations with increasing amplitude. Changes in some parameters which increase static stability may reduce the dynamic stability and vice versa. Second, from an engineering point of view, it is not only important to maintain system stability, but a certain degree of stability (stability margin) is necessary. For example, a system that is stable but highly oscillatory may be difficult to control.

A good example of these points is the handling of a vehicle without a trailer. In a steady-state turn, the yaw rate of the vehicle, ω_1, is

$$\omega_1 = \frac{v_x \delta}{l_1 + K_u v_x^2} \tag{10}$$

Here, l_1 is the vehicle wheel-base. The understeer gradient, K_u, is given by [14]

$$K_u = \frac{m_1\left(C_{yr}b_1 - C_{yf}a_1\right)}{C_{yf}C_{yr}l_1} = \frac{1}{g}\left(\frac{W_f}{C_{yf}} - \frac{W_r}{C_{yr}}\right) \tag{11a,b}$$

In the above, $W_{f/r}$ denote the front and rear axle static loads (due to gravity forces) and g is the gravity acceleration. If the understeer gradient is negative, vehicle yaw response diverges when the vehicle speed is above the critical speed $\sqrt{-l_1/K_u}$. Thus, increasing the understeer gradient improves static (steady-state) stability of the vehicle.

At the same time, since the vehicle model is a 2nd order system, which is typically under-damped throughout most of the speed range, it is characterized by the natural frequency and the damping ratio. The latter, which is a good indicator of dynamic stability, is given by the following function of speed [14]

$$\zeta(v_x) = \frac{\zeta_0}{\sqrt{1 + v_x^2\left(K_u / l_1\right)}} \tag{12}$$

Here, ζ_0 represents the damping ratio at zero speed. Hence, the larger the understeer gradient is, the faster the rate at which the damping coefficient decreases with speed. At sufficiently high speed, the yaw response of the vehicle can become highly oscillatory when K_u is large. While increasing the understeer gradient improves static stability, it can reduce dynamic stability at high speeds.

STATIC STABILITY – In order to study the static stability of a vehicle-trailer combination, the system described by equation (4) without the control and steering inputs is considered in steady-state condition (d**x**/dt = 0). That is

$$\mathbf{D}(v_x)\mathbf{x} = \mathbf{0} \tag{13}$$

Solving the above equation yields the steady-state values of the state variables. In particular, vehicle yaw rate, ω_1, is given by

$$\omega_1 = \frac{v_x \delta}{l_1 + \left(K_u - \Delta K_u\right)v_x^2} \tag{14}$$

K_u is the understeer gradient of the vehicle alone and ΔK_u is the change in the understeer gradient due to the presence of trailer. It is given by

$$\Delta K_u = \frac{m_2 b_2 \left[C_{yf}(a_1 + c_1) + C_{yr} e_1 \right]}{C_{yf} C_{yr} l_1 l_2} \qquad (15)$$

By observing that the changes in the static vertical loads of the vehicle front and rear axles due to the vertical hitch load are

$$\Delta W_f = -\frac{m_2 b_2 e_1 g}{l_1 l_2}; \quad \Delta W_r = \frac{m_2 b_2 (e_1 + l_1) g}{l_1 l_2} \qquad (16)$$

it can be shown that the understeer gradient of the vehicle trailer combination is given by

$$K_u - \Delta K_u = \frac{1}{g}\left(\frac{W_{ft}}{C_{yf}} - \frac{W_{rt}}{C_{yr}} \right) \qquad (17)$$

$W_{ft} = W_f + \Delta W_f$ and $W_{rt} = W_r + \Delta W_r$ are the static loads of the front and rear vehicle axle, respectively, when a trailer is present. Thus, equations (14) and (17) are identical to the corresponding equations for the vehicle without a trailer. It follows from equations (15) or (17) that the understeer gradient is reduced, as compared to that of the vehicle alone, when $b_2 > 0$ (i.e. when center of mass of the trailer is ahead of the trailer axle), it increases when $b_2 < 0$ and remains the same when $b_2 = 0$. Thus in a typical case of $b_2 > 0$, the presence of a trailer reduces the static stability of the articulated vehicle and increases steady state yaw response. It should be noted, however, that contrary to what is often assumed, the cornering stiffness values do not remain constant, but change with the changes in axle normal load. If the change in cornering stiffness were proportional to the normal load, there would be no change in the understeer gradient regardless of the dimension b_2. In reality, the cornering stiffness values change less than proportionally with normal load [14], resulting in changes in understeer gradient, which are directionally the same, but significantly smaller than those predicted under the assumption of constant cornering stiffness values.

DYNAMIC STABILITY – In order to study the inherent dynamic stability of a vehicle-trailer combination, consider a state equation of the free system (i.e. equation (6) with the control and steering inputs both equal to 0) under the assumption of constant speed:

$$\dot{\mathbf{x}} = \mathbf{A}\mathbf{x} \qquad (18)$$

The system eigenvalues (poles) are the eigenvalues of matrix **A**, that is, the roots of the characteristic equation

$$\det(s\mathbf{I} - \mathbf{A}) = 0 \qquad (19)$$

Here, **I** denotes an identity matrix and *s* is the Laplace operand which is the unknown variable in equation (19). Since **A** is a matrix of dimension 4x4 with all real coefficients, equation (19) is a 4-th order equation with real coefficients. The roots are therefore either real or complex occurring in conjugate pairs. For the system to be asymptotically stable, all the roots must have negative real parts. If any of the roots has a positive real part, the system becomes unstable. Since matrix **A** is speed dependent, the positions of the eigenvalues also change with speed. A convenient way of visualizing the changes in system eigenvalues and the degree of stability with speed is to plot the damping coefficients and the damped natural frequencies as functions of vehicle speed. If the system has a complex pair of poles at

$$s_{1,2} = -d \pm j\omega_d \qquad (20)$$

where *j* is the imaginary unit, *d* is the damping coefficient, and ω_d is the damped natural frequency, then the damping ratio, ζ, and the un-damped natural frequency, ω_n, are

$$\varsigma = \frac{-d}{\sqrt{d^2 + \omega_d^2}}, \quad \omega_n = \sqrt{d^2 + \omega_d^2} \qquad (21)$$

A negative damping ratio ζ indicates an unstable system. As a 4-th order system, the vehicle with trailer model has 2 pairs of complex conjugate poles with one damping ratio for each pair for the total of two. In contrast, the vehicle without trailer possesses only one pair of complex conjugate poles and one damping ratio. The damping ratios for the vehicle alone and the vehicle with trailer are plotted as functions of speed in Figure 2. The numerical values of parameters correspond to a large pick-up truck with a 2000 kg (~ 4400 lbs) trailer.

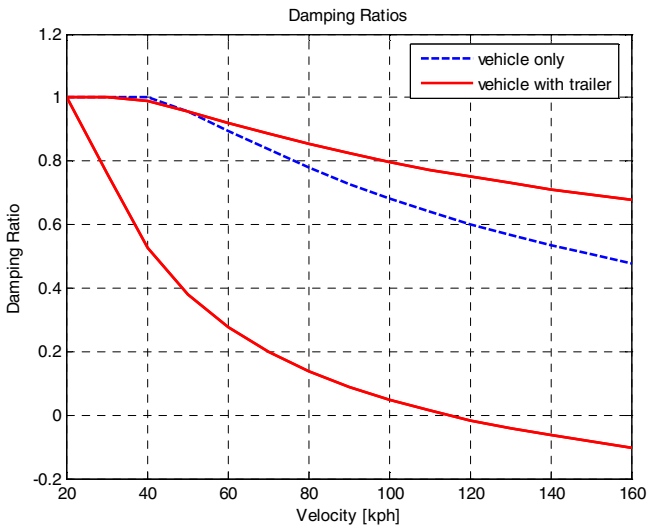

Figure 2: Damping Ratios of Vehicle Alone and Vehicle with Trailer as Functions of Speed

The vehicle without a trailer has the damping ratio which decreases with speed from 1 to about 0.5 at 160 kph (~ 100 mph), implying well damped response in the entire range of speeds. For the vehicle with trailer, one pair of eigenvalues has a slightly higher damping ratio than for the vehicle alone. The other pair of eigenvalues, in contrast, has a low damping ratio (below 0.3) at speeds above 60 kph (~ 37 mph); it becomes negative at about

115 kph (~ 71 mph), indicating that at or above this speed, the model of a vehicle with trailer becomes unstable. In the speed range between 60 kph (~ 37 mph) and 115 kph (~ 71 mph), the vehicle with trailer will exhibit oscillatory response, but with oscillations slowly decreasing with time. Above 115 kph (~ 71 mph), the oscillations initiated by any driver input or external disturbance will grow exponentially.

The model of vehicle with trailer was used to study the influence of various parameters on stability of a vehicle-trailer combination. For example, the distance b_2 of the trailer center of gravity to the trailer axle depends on the payload distribution. The effects of this distance on the damping ratio and the damped natural frequency of the least damped mode of the vehicle-trailer combination at the speed of 80 kph (~ 50 mph), are shown in Figure 3. The negative distance indicates that the center of gravity is behind the axle. The natural frequency does not change dramatically, but the damping ratio of the least stable mode decreases significantly as the center of gravity moves to the rear of the trailer, making the system less stable in the dynamic sense. Since moving the center of gravity rearward improves static stability, generally an optimal range of distance b_2 (and corresponding hitch load) is recommended.

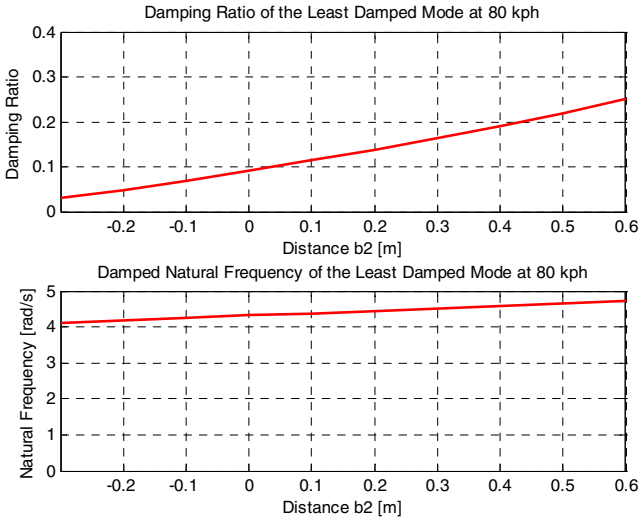

Figure 3: Damping Ratios and Damped Natural Frequency of the Least Damped Mode of Vehicle as Functions of Distance b_2 at Vehicle Speed of 80 kph

STABILIZATION THROUGH ACTIVE CONTROL

In this section, the effects of two control strategies using braking of the towing vehicle on stability of the vehicle-trailer combination are analyzed. The first one is slowing down the vehicle by symmetric braking until the vehicle speed drops significantly below the critical speed where natural damping of the system is sufficiently large. The second is the direct yaw moment control of the towing vehicle via asymmetric braking, which influences eigenvalues of the closed loop system; it is therefore capable of increasing damping in the system at any speed.

SYMMETRIC BRAKING – In this approach, the natural damping of the system is utilized, which changes gradually with speed, as indicated in Figure 2. Hence, vehicle speed has to be significantly reduced from the critical speed, before the damping in the system is sufficiently large to effectively damp the oscillations. In addition, braking of the towing vehicle without the trailer braking has the following second-order effects on the yaw dynamics of the system:

1) It introduces longitudinal inertial force at the trailer center of mass, which creates a destabilizing moment acting on the trailer (that is, a moment that tends to increase the hitch angle, θ);
2) It changes the normal loads of the vehicle and trailer axles, which in turn affect the cornering stiffness values for each axle;
3) It produces tire slips of front and rear axles of the towing vehicle which tend to reduce the lateral cornering stiffness of these axles.

The last effect depends on brake proportioning, but is generally small during light and moderate braking. The first two effects can be analyzed using the 4-th order model (equation 6) with the following modifications. First, the inertial force of the trailer, $-m_2 a_{x2}$, causes a corresponding longitudinal reaction force in the hitch joint, which affects equation (1d) describing the yaw motion of the trailer. This equation becomes

$$I_{z2}\dot{\omega}_2 = Y_h a_2 - F_{yt} b_2 - m_2 a_2 a_{x1}\theta \qquad (22)$$

Here, a_{x1} is longitudinal acceleration of the vehicle, which within the linear approximation is the same as that of the trailer. In addition, the changes in tire cornering stiffness (per axle) resulting from the normal load transfer from braking can be included in the model using quasi-static equations. Consequently, the system equation (4) takes the form

$$\mathbf{M}\dot{\mathbf{x}} = \mathbf{D}(v_{x1}, a_{x1})\mathbf{x} + \mathbf{E}u + \mathbf{F}\delta \qquad (23)$$

in which the matrix **D** is now a function of not only longitudinal speed, which is now time varying, but also longitudinal acceleration.

Even though the method of determining stability of a vehicle by investigating the location of eigenvalues applies strictly only to time invariant systems, this approach can be used when the system parameters vary slowly in time. Under this assumption, the critical speed of the vehicle (i.e. the speed at which the system comprising the vehicle and trailer becomes unstable) was determined at different levels of vehicle deceleration. The results are shown in Figure 4.

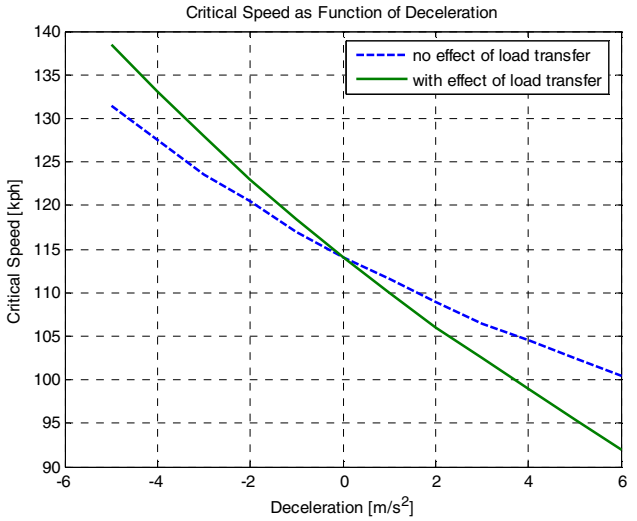

Figure 4: Critical Speed of Vehicle-Trailer Combination as a Function of Deceleration

In the figure, deceleration is positive and acceleration is negative. The dotted line represents the results obtained from the model (23), in which the effect of deceleration on cornering stiffness is not included, while the results depicted by the solid line include this effect. In both cases the critical speed is decreasing as deceleration increases. Thus the secondary factors decrease dynamic stability of the system during uniform braking.

DIFFERENTIAL BRAKING – In contrast, differential braking can directly affect the system eigenvalues at any speed. Within the model considered here, differential braking is modeled as a direct yaw control input applied to the towing vehicle. Let the output feedback control law be

$$\mathbf{u} = -\mathbf{K}(v_x)\mathbf{y} = -\mathbf{K}(v_x)\mathbf{C}\mathbf{x} \qquad (24)$$

Here, **y = Cx** is the output vector and **K** is the control gain matrix, which may be speed dependent. Then the closed loop system is described by the state equation

$$\dot{\mathbf{x}} = (\mathbf{A} - \mathbf{K}\mathbf{C})\mathbf{x} \qquad (25)$$

The eigenvalues of the closed loop system are the eigenvalues of matrix **A-KC**, which in general are different from those of the matrix **A**, corresponding to the original system. Using equation (25), the closed loop system eigenvalues and stability robustness with respect to parameter variations can be investigated for various control laws. Consequently, a control law can be selected, which uses only available signals while providing good robustness properties.

TRAILER TESTING AND SIMULATION

Using a custom built trailer, a series of experiments were performed to investigate sway characteristics at varying speed and loading conditions. To perform this stability investigation and to validate the earlier analysis, both real-world testing and simulation tools based were employed. The simulation model comprehends full vehicle and trailer dynamics including nonlinear characteristics, thus removing most limitations of the simpler analytical model. The trailer was designed to facilitate variation of stability properties in a wide range through changes in critical parameters.

TEST RIG - Trailer testing was conducted with a custom designed test trailer. The trailer, shown in Figure 5, can be altered for a variety of loading conditions. This flexibility offered by the trailer allows trailer sway motion to be induced at a large range of speeds and therefore promote safe testing scenarios and assist in stability and control robustness studies.

Figure 5: Test Trailer

The key feature which offers loading flexibility is an adjustable axle carriage. It features two axles, providing flexibility to mount wheels on one or both axles. More importantly, the carriage can be moved in one of five locations along the length of the trailer. Moving the axle carriage affects the trailer's Center of Gravity (CG) location, thus affecting its dynamic response. Furthermore, if additional ballast is required, an open frame design with mounting holes allows that ballast to be secured to the trailer at any location.

Three primary safety features are incorporated in the trailer design. The first feature is an electro-hydraulic braking system. A Tekonsha Prodigy brake controller installed in the towing vehicle controls a hydraulic pump mounted to the axle carriage. Based on voltage input from the brake controller, the pump supplies hydraulic pressure to vented, 4-piston caliper, disc brakes at each hub. In addition to the trailer brakes, there are devices designed to reduce the risks of roll-over and jack-knifing. To prevent roll-overs during extreme test maneuvers, outriggers are attached to mounting plates which are integrated into the trailer construction. In order to reduce the risk of jack-knifing, tow straps linking the trailer tongue to the outer, rear corners of the towing vehicle are used to limit the hitch angle to ~ 30°.

Instrumentation is mounted directly to the trailer to sense and process its dynamic motions. An inertial

measurement unit and optical Datron sensor are used to measure yaw rate, lateral acceleration, and lateral and longitudinal velocities. The sensors are routed to a dSPACE MicroAutobox which processes and transmits the signals through CAN to a second MicroAutobox mounted in the towing vehicle, which is also equipped with similar dynamic motion sensors. Therefore, both vehicle and trailer data can be acquired simultaneously with the same data file.

RESULTS – In this section, the results from testing and simulation are reported. Experiments were performed with the axle carriage in one of two locations. Position A is with the carriage in its "home" position, that location which is recommended by the trailer manufacturer for normal towing operation. Position B is with the carriage in its most forward location. The following list provides a brief description of configurations considered in this paper. For each configuration, a 4 inch (~ 10 cm) drop ball mount was used for securing the trailer to the towing vehicle's receiver.

- *Position A, Tandem Axle:* Axle carriage is at its home position, Position A, with tires mounted to both axles.
- *Position B, Single Axle:* Axle carriage is at its most forward position, Position B, with tires removed from the front axle.
- *Position B, Tandem Axle:* Axle carriage is at its most forward position, Position B, with tires mounted to both axles.

Static Loading and Tire Cornering Stiffness – To support the results documented for each configuration in the following sections, static loading conditions and tire cornering stiffness data is provided. The figures for static loading illustrate tire normal loads, tongue loading, and dimensional characteristics of the vehicle-trailer combination for a given configuration. From this information, the locations of the resultant axle load and trailer center of gravity are determined and also displayed. Additionally, data is presented to explain the lateral force capability, which is affected by changes in static loading.

Static loading conditions for the three configurations are detailed in figures 6, 7, and 8. In Figure 6, the static loading conditions for Position A, Tandem Axle are shown. The tongue load is 283 lbs (~ 1260 N), which follows general towing guidelines that the tongue weight should be ~ 10 – 15% of the total trailer weight. With this configuration, the trailer CG is located 148 inches (~ 376 cm) from the hitch point, and it is ~ 17 inches (~ 43 cm) in front of the resultant tire load which acts at 164.5 inches (~ 418 cm) from the hitch point. Next, the static loading conditions for Position B, Single Axle are shown in Figure 7. Compared to Position A, Tandem Axle, the tongue load is significantly reduced at 85 lbs (~ 378 N), and there is a slight increase in the normal load acting at the trailer axle. The trailer center of gravity location is shifted forward on the trailer, but the axle load is shifted even more, resulting in the distance between the two (b_2) of only 4 inches (~ 10 cm). Finally, static loading for Position B, Tandem Axle is shown in Figure 8. Simply re-mounting the tires to the front axle has significant effects on the b_2 distance and tongue loading. The weight transfer from the vehicle onto the trailer results in a negative tongue load of -280 lbs (~ - 1247 N). While the CG location changes by only one inch, the resultant tire normal load moves forward by 17 inches (~ 43 cm). As a result, the trailer CG is now located 12 inches (~ 30 cm) behind the resultant axle load. As predicted by the analytical model and as will be shown in test results, this has an adverse effect on trailer dynamic stability.

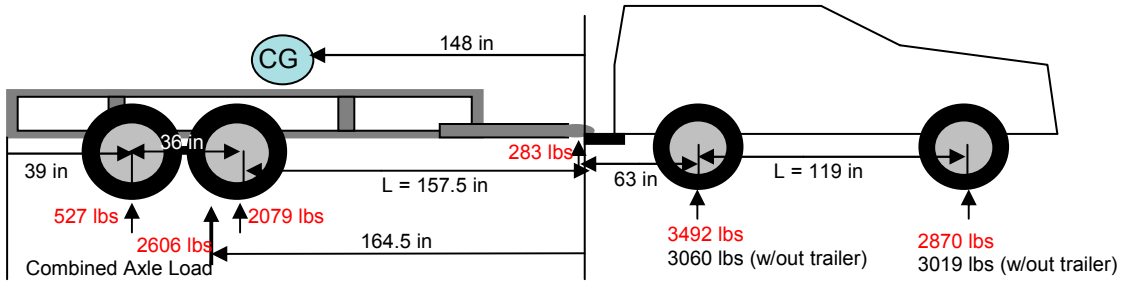

Figure 6: Static Loading – Position A, Tandem Axle

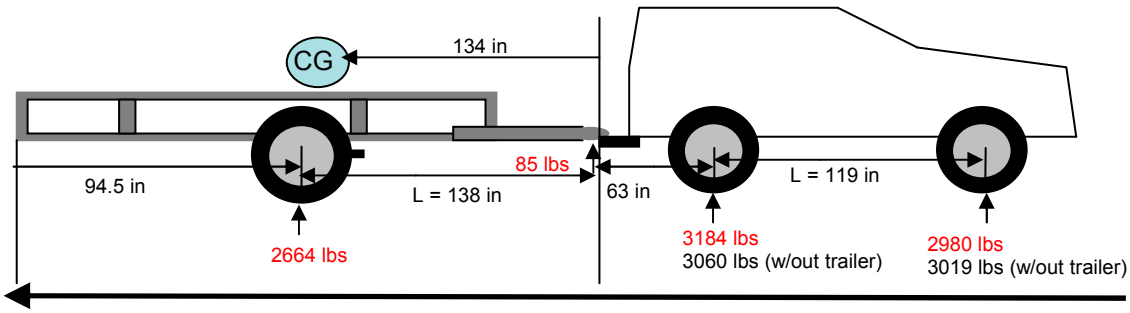

Figure 7: Static Loading – Position B, Single Axle

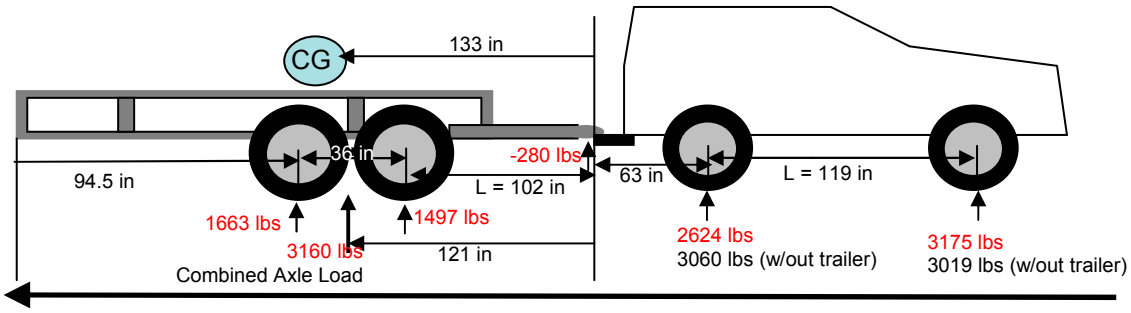

Figure 8: Static Loading – Position B, Tandem Axle

It is necessary to characterize tire lateral force of the trailer and cornering stiffness to provide modeling accuracy for simulations and to comprehend the effect of loading on lateral capability. Determining the tire lateral force characteristics requires a plot of tire lateral force vs. tire slip angle (α). For this paper, all such plots combine the lateral tire forces for all trailer tires into a single total force vector for the trailer, as was done in the analytical model. Lateral force and slip angle data for the trailer tires was obtained by subjecting the vehicle-trailer system to a steady state cornering maneuver until the point of maximum achievable lateral acceleration was reached. To achieve this, a slowly increasing steer maneuver was performed on dry asphalt at 30 mph (~ 48 kph). During the maneuver, lateral acceleration and yaw rate were measured at the trailer's center of gravity (CG) using the inertial measurement unit. With this information, the combined lateral tire force can be calculated by solving equations (1c) and (1d) for the unknown lateral hitch and tire forces, Y_h and F_{yt}. Since under steady-state conditions $\dot{b}_2 = 0$, this yields

$$F_{yt} = \frac{m_2 a_2}{a_2 + b_2} a_{y2} \qquad (26)$$

The Datron sensor measurement of trailer lateral velocity (at CG), v_{y2}, and longitudinal velocity, v_x, can be combined with the yaw rate data to estimate tire slip angle, , as follows

$$v_{yt} = v_{y2} - b_2 \omega_2, \quad \alpha = \tan^{-1}\left(\frac{v_{yt}}{v_x}\right) \qquad (27)$$

where v_{yt} is the lateral velocity translated to the resultant tire load location.

Combined tire cornering stiffness values were determined by applying the above series of equations to data captured during the slowly increasing steer maneuver. Lateral force characteristics for each of the three configurations are plotted in Figure 9. They were obtained by a least square curve fitting method, in which a parabolic curve was forced to pass through the origin.

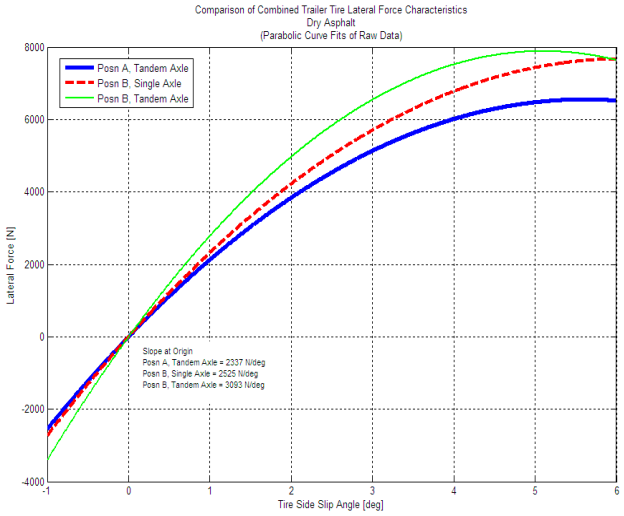

Figure 9: Lateral Tire Force vs. Slip Angle – Comparison of Three Trailer Configurations

For characterization purposes, a critical parameter is the cornering stiffness, which is the slope of the curve at 0° of slip angle (α). It is important to note that this value is a function of many parameters which include, but are not limited to, loading condition, tire pressure, tire-road surface friction, and suspension stiffness and damping. The cornering stiffness is 2337 N/deg for Position A, Tandem Axle; it is 2525 N/deg for Position B, Single Axle, and 3093 N/deg for Position B, Tandem Axle. Since the normal tire loads are 2606 lbs (~ 11,590 N), 2664 lbs (~ 11,850 N), and 3160 lbs (~ 14,060 N), it is apparent that the cornering stiffness increases with normal load, but is not significantly affected by the number of axles.

SIMULATION VALIDATION Simulations of the nonlinear full vehicle with trailer model were performed using the CarSim® environment. The accuracy of the model was verified by comparing simulation results with test data collected on a base truck (no active systems) towing a trailer. For each trailer loading configuration (Position A or B), the axle and hitch loads in the vertical direction were first validated against test data collected at the static equilibrium condition by adjusting the center of gravity location of the tractor and trailer. The tire data collected based on the single axle trailer loading configuration was used to represent the lateral force dynamics of the trailer.

As an example, comparisons between the test data (solid line) and simulation (dashed line) for the steering wheel input, vehicle speed, yaw rate, and lateral acceleration of both the vehicle and trailer are shown in Figure 10 for trailer configuration in Position B, Single Axle. The figure demonstrates that the simulation model matches well with the test data. The model was also validated for other trailer configurations demonstrating very good agreement with experiments in predicting the onset of instability.

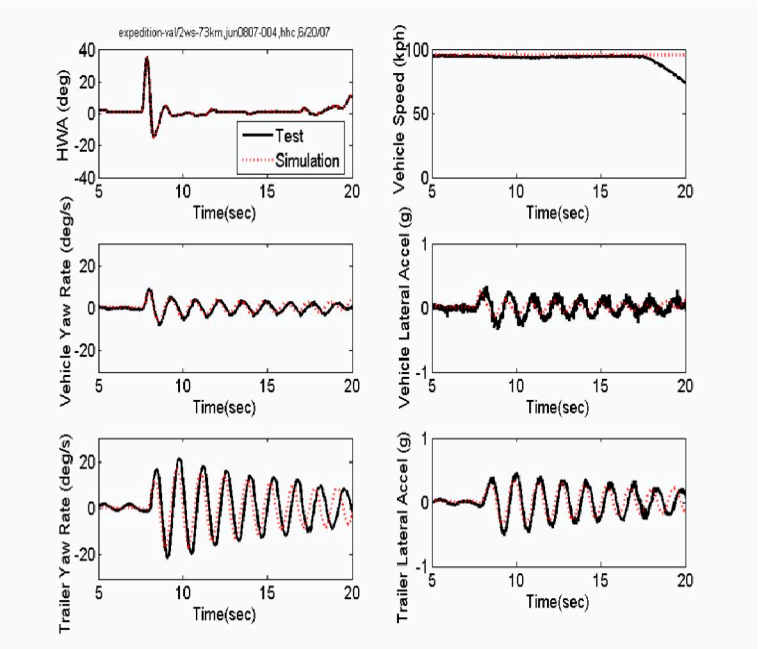

Figure 10: Model Validation for Position B, Single Axle

TRAILER RESPONSE – First, the trailer response was characterized for Position A, Tandem Axle (configuration used for normal towing activity). Both analysis and simulation of a validated vehicle-trailer model representing this configuration revealed stable response across a wide band of speeds. The selected results of simulations performed at several speeds are displayed in Figure 11. In the figure, the top two plots show yaw rate and lateral acceleration data for the vehicle, and the bottom plots show the same variables for the trailer. The simulation used an impulse steering input to disturb the system and induce dynamic response. At speeds less than 100 kph (~ 62 mph), the response dampens out within a couple of cycles. As speed increases, greater amplitudes of oscillations are present in the trailer data as well as decreased damping. Even at 160 kph (~ 100 mph), though, the system is still fairly well damped. In part, the stability of this particular system can be attributed to increased lateral force capability at the towing vehicle's rear axle. The positive tongue load of 283 lbs (~ 1260 N) increases the combined rear axle normal load by ~ 400 lbs (~ 1780 N). Position A offers the widest dynamic stability margin of the three configurations tested and documented in this paper. Furthermore, due to the high speeds required to induce instability for this condition, road testing for trailer sway was not conducted for safety reasons.

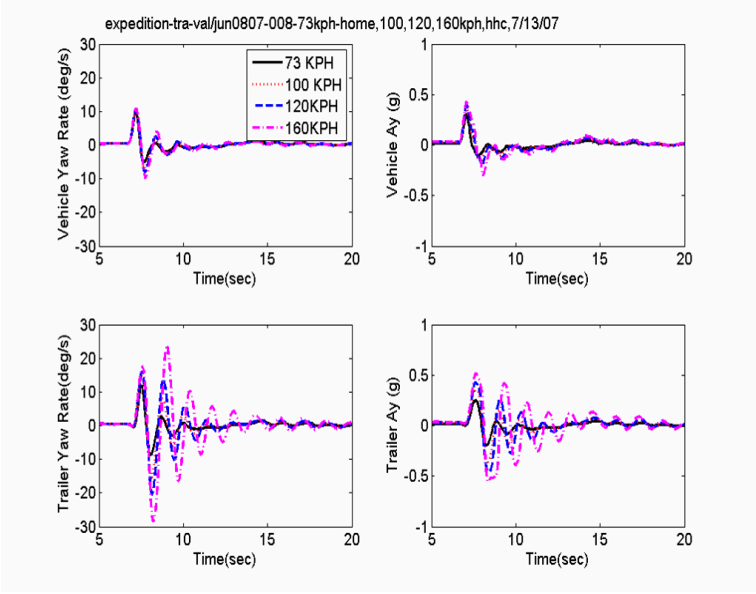

Figure 11: Simulation Results – Position A, Tandem Axle

To facilitate road testing of trailer sway at relatively low speeds, the axle carriage was moved to its most forward position (Position B). The front tires were removed to create a single axle configuration. A series of straight-line tests were conducted on a vehicle dynamics pad at varying speeds. Once a steady state condition was reached in which the vehicle-trailer combination was traveling straight at the desired speed, an impulse steering input of ~ 50° from the towing vehicle was applied to disturb the system and induce trailer oscillation. The results obtained for the minimum and maximum speeds tested for this configuration are shown in Figure 12. The longitudinal speed, yaw rate, and estimated hitch angle for the trailer are displayed. In addition, a plot of the towing vehicle's steering wheel angle is included to provide a frame of reference on when the disturbance was introduced. Whereas the amplitude of each signal provides detail on the severity of the maneuver, noting the damping effects is of greater importance for characterizing the stability margin. At 72kph (45mph), shown by the solid line, the oscillations are fully damped within ~ 10 seconds. For 96kph (60mph), shown by the dashed line, the output signal amplitudes are ~ 50% greater. Although the system is still damped, it takes almost twice as long for the sway motion to cease. The frequency of oscillations for both speeds, though, is similar. Recall that the analytical model predicts that the damping ratio decreases as distance b_2 (measured from the trailer CG to the resultant axle load) decreases. Although Position B, Single Axle generates a higher cornering stiffness value than Position A, b_2 is much smaller (4 inches (~ 10 cm) vs. 17 inches (~ 43 cm)). As a result, oscillations with higher amplitudes and less damping are observed at lower speeds.

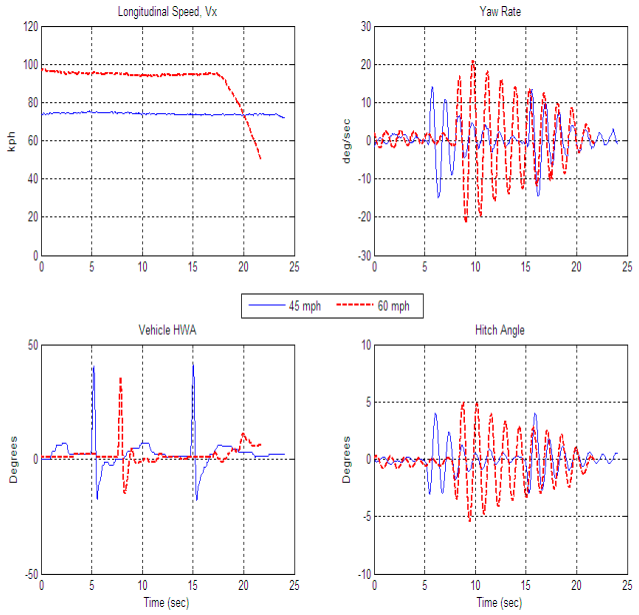

Figure 12: Trailer Sway Test Results – Position B, Single Axle

To augment the road testing, simulation was employed to determine the critical speed at which this vehicle-trailer combination becomes unstable. Simulation results for three speeds: 96kph (60mph), 100kph (62mph), and 104kph (65mph) are shown in Figure 13. The simulations used the same steering input disturbance that was applied during testing. As with the test data, the simulation shows the vehicle-trailer combination to have oscillatory response at 96kph (60 mph), but it eventually leads to a stable equilibrium condition. However, as speed is increased to 104kph (65mph), the system becomes unstable due to the onset of a negative damping condition. The critical speed predicted by the linear analytical model is virtually identical.

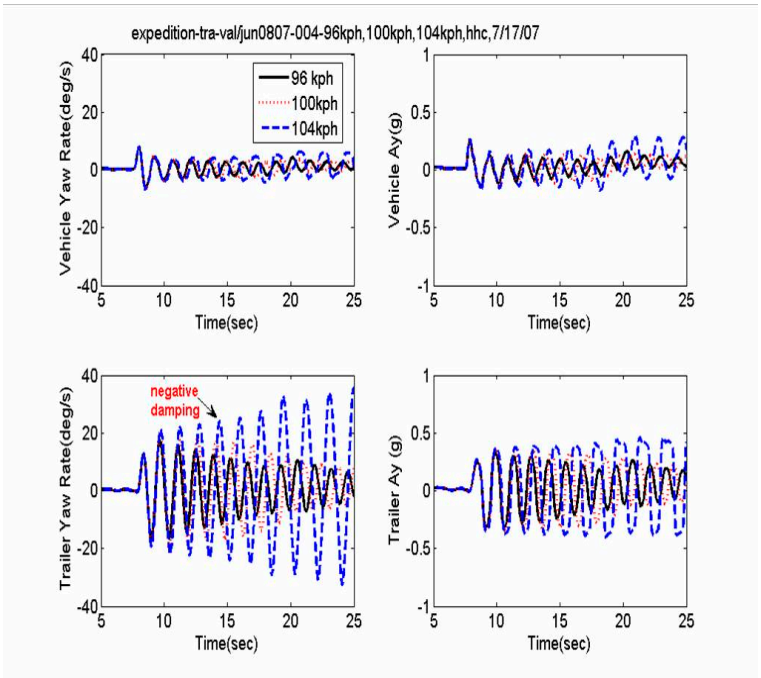

Figure 13: Simulation Results – Position B, Single Axle

Using the same axle carriage position, Position B, tests were performed with a tandem axle set-up to compare against the single axle configuration. The trailer dynamic responses for speeds of 48kph (30mph) and 72kph (45mph) are shown in Figure 14. For the tandem axle, 72kph (45mph) appears to be the critical speed at which the system becomes marginally stable. Shown with the dashed line, the amplitude for yaw rate remains almost constant as time continues beyond the initial disturbance. Thus, the static loading conditions have a substantial impact on the critical speed at which the sway motion becomes unstable.

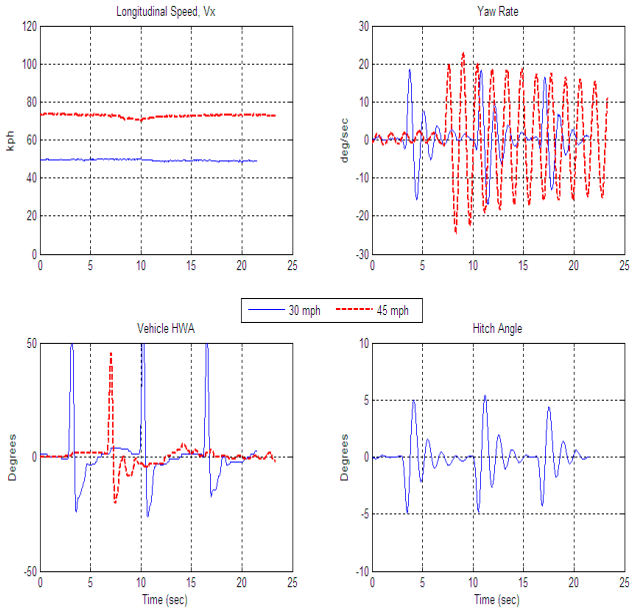

Figure 14: Trailer Sway Test Results – Position B, Tandem Axle

The lack of hitch angle data for the 72kph (45 mph) trace is the result of severity of oscillations. Since the calculation of this angle relies on integration of yaw rate data from the IMU sensors, it is necessary to account for yaw rate sensor biasing to remove errors that build over time. To determine the bias factors, the vehicle-trailer combination must be driven in a straight line without any actual yaw rate at the beginning and end of the run. Due to test surface size limitations, it was not possible to obtain a zero yaw condition at the end of the run for Position B, Single Axle tested at 72kph (45 mph) because of persistent oscillations. Hence, an accurate estimation of hitch angle could not be determined.

SUMMARY – The key parameters and results of the three trailer configurations analyzed here are summarized in Table 1. Those items are the resultant axle normal load, combined trailer tire cornering stiffness, center of gravity location with respect to resultant axle load (distance b_2), and the critical speed at which the sway motion becomes unstable. Cornering stiffness increases as axle normal load increases. However, there is not a direct correlation between cornering

stiffness and critical speed. The primary indicator of achievable critical speed is the b_2 distance. As that distance decreases or even becomes negative when the CG is located behind the axle load, trailer stability is adversely affected and instability occurs at lower speeds, as predicted by the analytical model.

Configuration	Resultant Tire Normal Load N (lbs)	Cornering Stiffness N/deg (lb/deg)	b_2 Distance m (inches)	Critical Speed kph (mph)
Position A Tandem Axle	11592 (2606)	2337 (525)	0.419 (16.5)	>160 (>100)
Position B Single Axle	11850 (2664)	2525 (568)	0.102 (4)	104 (65)
Position B Tandem Axle	14056 (3160)	3093 (695)	-0.305 (-12)	72 (45)

Table 1: Data Summary Table

SWAY CONTROL METHODS

The validated simulation model (Position B, Tandem Axle) is used to study advantages and limitations of two active brake control methods: the uniform braking and the direct yaw moment (DYM) control of the towing vehicle. In both methods, only signals available from the towing vehicle ESC system are utilized. The driver starts with initial speed of 73 kph (45 mph), and the system is subject to a sine wave steer input with magnitude of 50° and frequency of 1Hz as shown in Figure 15.

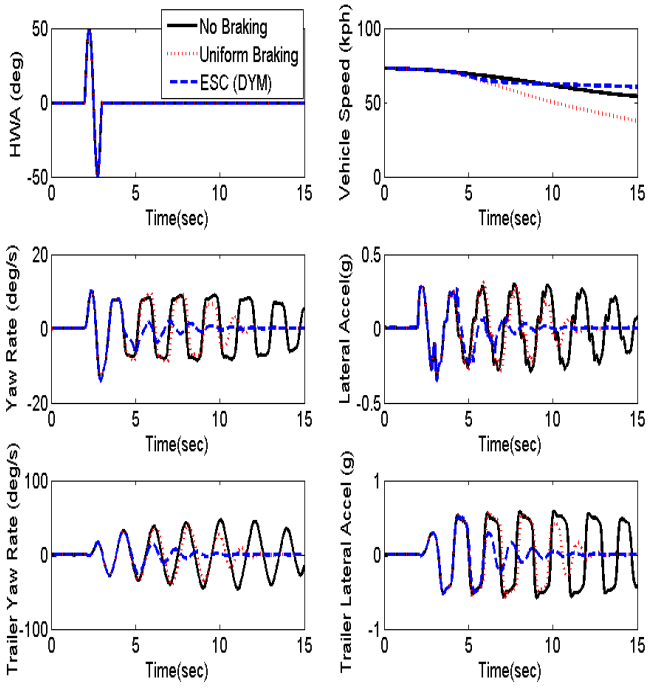

Figure 15: Effects of Two Active Brake Control Methods on Trailer Stability – Position B, Tandem Axle (No Throttle)

No throttle input is applied. The base vehicle-trailer configuration (designated as No Braking) exhibits highly oscillatory yaw rate and lateral acceleration responses of both the vehicle and the trailer. The direct yaw moment control based on towing vehicle asymmetric braking significantly enhances the directional stability of the vehicle-trailer combination. The uniform braking control on the towing vehicle effectively reduces the vehicle speed. However, it takes a longer time (10 seconds after brake is applied) to damp out the vehicle and trailer yaw rate and acceleration responses. As shown in Figure 16, when the throttle input is applied to maintain a constant vehicle speed of 73 kph (45 mph) in the maneuver without braking, the trailer's yaw rate of the "No Braking" configuration leads to a dynamic instability (i.e., negative damping). Once again, the direct yaw moment control (coarse dashed line) significantly enhances the vehicle and trailer yaw stability as compared to the uniform braking control (dashed line).

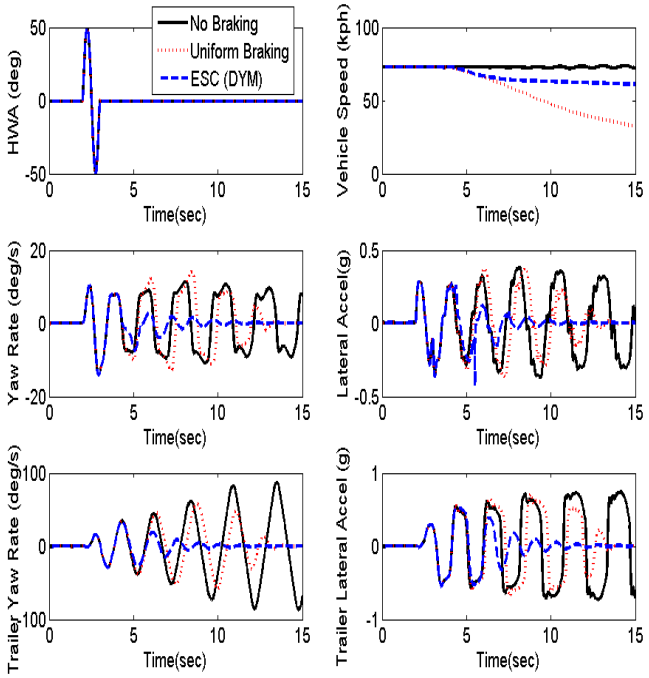

Figure 16: Effects of Two Active Brake Control Methods on Trailer Stability – Position B, Tandem Axle (With Throttle)

CONCLUSIONS

In this paper, the investigation of snaking oscillations of a vehicle-trailer combination is documented. Analytical modeling, simulation, and road testing were used to study dynamic response as it is affected by various speed and loading conditions. Furthermore, a brief analysis of control methods for suppressing the oscillation using only brake actuators and sensors from the towing vehicle ESC system is presented. Results of the experimentation performed give rise to the following conclusions:

1. The analytical model provides good description of dynamic behavior of the vehicle-trailer combination; it can be used to accurately predict the onset of snaking oscillations and to study the effects of system parameters on stability.
2. The test trailer proved to be an effective tool at creating the desired testing scenarios.
    a. Dynamic behavior of the trailer can be significantly altered without adding more weight.
    b. Instability could be induced at low speeds which promotes a safe testing environment.
3. Results of the experiments performed on the road conform to those learned through analytical modeling and simulation.
4. The trailer's center of gravity location relative to its resultant axle load location is a critical factor in trailer stability.
    a. Small variations in CG location fore or aft of the resultant tire normal load have significant effects on achievable speed and stability levels.
    b. In the cases shown here, trailer stability appears to be more dependent on CG location than on trailer tire cornering stiffness.
5. Control strategy involving direct yaw moment via asymmetric braking of towing vehicle is more effective in stabilizing the snaking oscillations than symmetric braking.
    a. Direct yaw moment control can damp oscillations without significant reduction in speed
    b. Symmetric braking can also stabilize the system, but it has negative second-order effects on system stability and requires large reduction in vehicle speed, significantly below the critical speed, to utilize natural damping in the system.

REFERENCES

1. Bundorf, R. T., 1967, "Directional Control Dynamics of Automobile-Travel Trailer Combination", *SAE paper No.* 670099, pp. 667-680.
2. Kurtz, E. F. and Anderson, R. J., 1977, Handling Characteristics of Car-Trailer Systems; A State-of-the-Art Survey", *Vehicle System Dynamics*, **6**, pp. 217-243.
3. Deng, W. and Kang, X., 2003, "Parametric Study on Vehicle-Trailer Dynamics for Stability Control", *SAE paper No.* 2003-01-1321.
4. Fratila, D. and Darling, J., 1995, "Improvements to Car/Caravan Handling and High Speed Stability Through Computer Simulation", *ASME Paper WA/MET*-9.
5. Bevan, B. G., Smith, N. P., and Ashley, C., 1983, "Some Factors Influencing the stability of Car/Caravan Combinations", *I. Mech. Eng. Conf. Publ.* 1983-5, MEP, London, pp. 221-227.
6. Anderson, R. J., Kurtz, E. F., 1980, "Handling Characteristics Simulations of Car-Trailer Systems", *SAE paper No.* 800545.
7. Kageyama, I. And Nagai, R., 1995, "Stabilization of Passenger Car-Caravan Combination using Four Wheel Steering Control", *Vehicle System Dynamics*, **24**, pp. 313-327.
8. Deng, W., Lee, Y. H., and Tian, M., 2004, "An Integrated Chassis Control for Vehicle-Trailer Stability and Handling Performance", *SAE paper No.* 2004-01-2046.
9. Lugner, P., Plochl, M., and Riepl, A., 1996, "Investigation of Passenger Car_Trailer Dynamics Controlled by Additional Braking of Trailer", *Proceedings from AVEC'96. International Symposium on Advanced Vehicle Control,* pp. 763-778.
10. Alonso Fernandez, M., A. and Sharp, R. S., 2001, "Caravan Active Braking System-Effective Stabilization of Snaking of Combination Vehicles", *SAE paper No.* 2001-01-3188.
11. Kimbrough, S., Elwell, M. and Chiu, Ch., "Braking Controllers and Steering Controllers for Combination Vehicles", *International Journal of Vehicle Design*, **1**(2), pp. 195-222.
12. Waldbauer, D. and Krober, J., 2006, "Method and System for Stabilizing a Car-Trailer Combination", US Patent Application Publication No. US 2006/0033308 A1.
13. Williams Jr., J. M. and Mohn, F.-W., 2004, "Trailer Stabilization through Active Braking of the Towing Vehicle", *SAE paper No.* 2004-01-1069.
14. Dixon, J. C., 1996, "*Tires, Suspension and Handling*", SAE, Inc., Warrendale, PA.

APPENDIX

Matrices in equation (6).

$$\mathbf{M} = \begin{bmatrix} m_1 + m_2 & -m_2(c_1 + a_2) & -m_2 a_2 & 0 \\ m_1 c_1 & I_{z1} & 0 & 0 \\ -m_2 a_2 & I_{z2} + m_2 a_2 (c_1 + a_2) & I_{z2} + m_2 a_2^2 & 0 \\ 0 & 0 & 0 & 1 \end{bmatrix} \quad \text{(A1)}$$

$$\mathbf{D}=\begin{bmatrix} -\dfrac{C_{yf}+C_{yr}+C_{yt}}{v_x} & \dfrac{-C_{yf}a_1+C_{yr}b_1+C_{yt}(c_1+l_2)-(m_1+m_2)v_x^2}{v_x} & \dfrac{C_{yt}l_2}{v_x} & C_{yt} \\ -\dfrac{C_{yf}(a_1+c_1)+C_{yr}e_1}{v_x} & \dfrac{-C_{yf}a_1(a_1+c_1)+C_{yr}b_1e_1-m_1c_1v_x^2}{v_x} & 0 & 0 \\ \dfrac{C_{yt}l_2}{v_x} & \dfrac{-C_{yt}l_2(c_1+l_2)+m_2a_2v_x^2}{v_x} & -\dfrac{C_{yt}l_2^2}{v_x} & -C_{yt}l_2 \\ 0 & 0 & 1 & 0 \end{bmatrix} \quad \text{(A2)}$$

$$\mathbf{E}=\begin{bmatrix} C_{yf} & 0 & 0 \\ C_{yf}(a_1+c_1) & 1 & 0 \\ 0 & 0 & 1 \\ 0 & 0 & 0 \end{bmatrix} \qquad \mathbf{F}=\begin{bmatrix} 1 & 1 \\ c_1 & 0 \\ 0 & -a_2 \\ 0 & 0 \end{bmatrix} \quad \text{(A3, A4)}$$

Matrices in equation (8)

$$\mathbf{A_v}=\begin{bmatrix} -\dfrac{C_{yf}+C_{yr}}{m_1v_x} & \dfrac{-C_{yf}a_1+C_{yr}b_1}{m_1v_x}-v_x \\ \dfrac{-C_{yf}a_1+C_{yr}b_1}{I_{z1}v_x} & -\dfrac{C_{yf}a_1^2+C_{yr}b_1^2}{I_{z1}v_x} \end{bmatrix},\ \mathbf{B_v}=\begin{bmatrix} 0 \\ \dfrac{1}{I_{z1}} \end{bmatrix},\quad \mathbf{G_v}=\begin{bmatrix} \dfrac{C_{yf}}{m_1} \\ \dfrac{C_{yf}a_1}{I_{z1}} \end{bmatrix} \quad \text{(A5)}$$